Melt–peridotite interactions in shallow mantle at the East Pacific Rise: evidence from ODP Site 895 (Hess Deep)

STEPHEN J. EDWARDS

Department of Environmental and Geographical Sciences, Manchester Metropolitan University, Chester Street, Manchester M1 5GD, UK

AND

JOHN MALPAS*

Department of Earth Sciences, Memorial University of Newfoundland, St. John's, Newfoundland A1B 3X5, Canada

Abstract

Ocean Drilling Program (ODP) Leg 147 recently drilled at Site 895 in Hess Deep (eastern Equatorial Pacific), where a structurally dissected section of the East Pacific Rise (EPR) is preserved, and intersected the mantle-crust transition zone of a fast-spreading centre for the first time. The core from Hole 895D (latitude 2°16.635'N, longitude 101°26.777'W) revealed that harzburgite is predominant over dunite in the top section of the Hole, but the reverse relationship is found lower in the section where dunite is closely associated with gabbroic rocks (gabbro and troctolite). Texture, mineralogy and mineral chemistry suggest a two-stage evolution for harzburgite preserved at the transition zone. Harzburgite with a porphyroclastic texture was produced by partial melting of peridotite to, or beyond the clinopyroxene-out phase boundary before or during asthenospheric (>1000°C) flow, which suggests a higher degree of mantle melting than normally expected below mid-ocean ridges. Subsequently, basaltic melt(s) interacted with this refractory harzburgite (olivine + orthopyroxene + spinel), which resulted in dissolution of orthopyroxene, re-equilibration and formation of olivine and spinel, and formation of clinopyroxene ± plagioclase, this is manifested as a progressive conversion of harzburgite to gabbroic rock through an intermediate dunite. At low melt/peridotite ratios, harzburgite was refertilised as the plagioclase component of the melt completely reacted with the peridotite matrix to produce clinopyroxene–spinel intergrowths and Al enrichment in ferromagnesian minerals. At high ratios, orthopyroxene completely dissolved incongruently, plagioclase appeared, and spinel was partially to completely resorbed; this produced olivine-bearing and olivine-free gabbroic rocks. Residual minerals in peridotites adjacent to gabbroic zones were enriched in Fe and Ti and depleted in Al.

KEYWORDS: harzburgite, mid-ocean ridge basalt, melt–peridotite interaction, mantle refertilization, Hess Deep, East Pacific Rise, ODP Leg 147.

Introduction

STUDIES of ophiolites, fragments of ancient oceanic lithosphere produced in a number of tectonic settings (Pearce *et al.*, 1984), have revealed the complexity of the sub-oceanic mantle and mantle-crust transition zone (Nicolas, 1989). Multiple episodes of melt generation and the migration of these melts through the mantle are recorded by the texture, mineralogy and chemistry of mantle peridotites (e.g. Quick, 1981; Evans, 1985; Duncan and Green, 1987; Nicolas, 1989; Kelemen *et al.*, 1992; Suhr and Robinson, 1994). Melt activity appears to be high at the mantle-crust transition zone (Nicolas, 1989; Suhr

* Present address: Department of Earth Sciences, University of Hong Kong, Pokfulam Road, Hong Kong.

Mineralogical Magazine, February 1996, Vol. 60, pp. 191–206

and Robinson, 1994), and not only are residues of partial melting and magmatic veins and dykes present at this level, but there is also abundant evidence of melt–peridotite interaction. The latter involved dissolution of orthopyroxene, formation of olivine, spinel, plagioclase and clinopyroxene, and textural and chemical re-equilibration of pre-existing olivine and spinel (e.g. Violette, 1980; Leblanc *et al.*, 1980; Nicolas and Prinzhofer, 1983; Nicolas, 1989; Edwards, 1991; Suhr and Robinson, 1994). This interaction has a profound influence on the composition of the mantle and the melts migrating through it (e.g. Quick, 1981; Evans, 1985; Fisk 1986; Kelemen 1990; Kelemen *et al.*, 1990, 1992; Elthon, 1992).

The exact nature and extent of melt–peridotite interaction depends on many factors. After a primary melt is produced, the chemical change it experiences as it migrates through the mantle towards the crust will depend on the extent of crystal fractionation and reaction with peridotite. Reaction depends on the degree of disequilibrium between the reacting components, the activity of fluids, the rate of melt migration, the ratio of melt volume to mineral surface area (the melt/peridotite ratio, i.e. massive intrusion, dyke, vein or grain boundary melt infiltration), and the extent of sealing reactions which isolate reacting components. The texture, mineralogy and mineral chemistry of peridotites should reflect some or all of these factors, provided that subsequent extreme physical and chemical re-equilibration has not occurred. Complications arise when (i) melt has passed through mantle peridotite causing significant modification but without fractionating any new phases, (ii) melt has interacted and fractionated simultaneously, and (iii) successive generations of melt of different composition have passed through the same column of mantle. It is usually only the most recent interactions which are unequivocally detectable in peridotites.

In the small number of samples of *in situ* sub-oceanic mantle available for study, evidence for melt–peridotite interaction is rare (Girardeau and Francheteau, 1993). However, peridotites sampled at Hess Deep on the eastern flank of the East Pacific Rise (EPR) by the submersible *Nautile* and by Ocean Drilling Program (ODP) Leg 147 do show the results of such processes (Gillis *et al.*, 1993; Girardeau and Francheteau, 1993; Hekinian *et al.*, 1993; Dick *et al.*, 1994). At Site 895, ODP Leg 147 recovered the first drill-core samples of transition zone upper mantle and lower crust originally formed at a fast-spreading centre. The significance of these unique samples cannot be overstated, and the present study integrates new textural, mineralogical and mineral chemical data obtained from samples from Hole 895D. These data are used to examine the effect of melt–peridotite interaction on the textural and chemical evolution of harzburgitic mantle at the mantle-crust transition zone of a fast-spreading centre. Detailed examination of the chemical evolution of mid-ocean ridge basaltic (MORB) melts during this interaction is beyond the scope of this study.

Geologic setting and previous work

Hess Deep (latitude 2°15′N, longitude 101°30′N) is the deepest portion of an oceanic rift valley that is propagating westward into the eastern flank of the EPR ahead of the Cocos-Nazca spreading centre (Figs. 1 and 2). Some 70 km east of the EPR axis, a median ridge in the rift valley exposes a structurally dissected section of the EPR which includes peridotites, gabbroic rocks, diabase dykes and volcanic rocks. Six holes were drilled at three different locations at Site 895 along the southern slope of the intra-rift ridge (Fig. 2), in an area where ultramafic rocks had previously been recovered during *Nautile* Dive 17 (Francheteau *et al.*, 1990). Harzburgite is the dominant lithology in Holes 895A-D and F, whereas dunite and gabbroic rocks are much more common in Hole 895E. Initial results from all Holes suggest a laterally heterogeneous mantle beneath the EPR prior to Hess Deep rifting. It has been suggested that such heterogeneity may have resulted from melt flow through the shallow mantle, with flow focused in a conduit sampled at Hole 895E (Gillis *et al.*, 1993; Dick *et al.*, 1994).

Hole 895D (latitude 2°16.635′N, longitude 101°26.777′W) penetrated 93.7 m of igneous basement below a water depth of 3820.7 m and recovered 21.4% of the drilled section (Fig. 3). Rock types sampled include harzburgite (77.9%), dunite (10.8%), gabbroic rocks (9.6%; comprising 5.4% troctolite and 4.2% gabbro) and basalt (1.7%) (Gillis *et al.*, 1993). Harzburgite is predominant over dunite in the top section of the Hole, but the reverse relationship is found lower in the section where dunite is closely associated with gabbroic rocks (gabbro and troctolite) (Fig. 3). With the exception of basalt, representative samples of each rock type have been investigated in the present study (Fig. 3 and Appendix I).

All rocks are highly altered and record greenschist to zeolite facies metamorphic conditions. In the ultramafic rocks, alteration is dominated by serpentine after olivine and by tremolite, bastite and chlorite after orthopyroxene. In mafic rocks, coronitic alteration of olivine and plagioclase is well developed where olivine is replaced by serpentine, tremolite and magnetite, and plagioclase by prehnite, chlorite, zeolite and hydrogrossular. Alteration of spinel is reflected by the development of magnetite and ferritchromit at grain boundaries and along

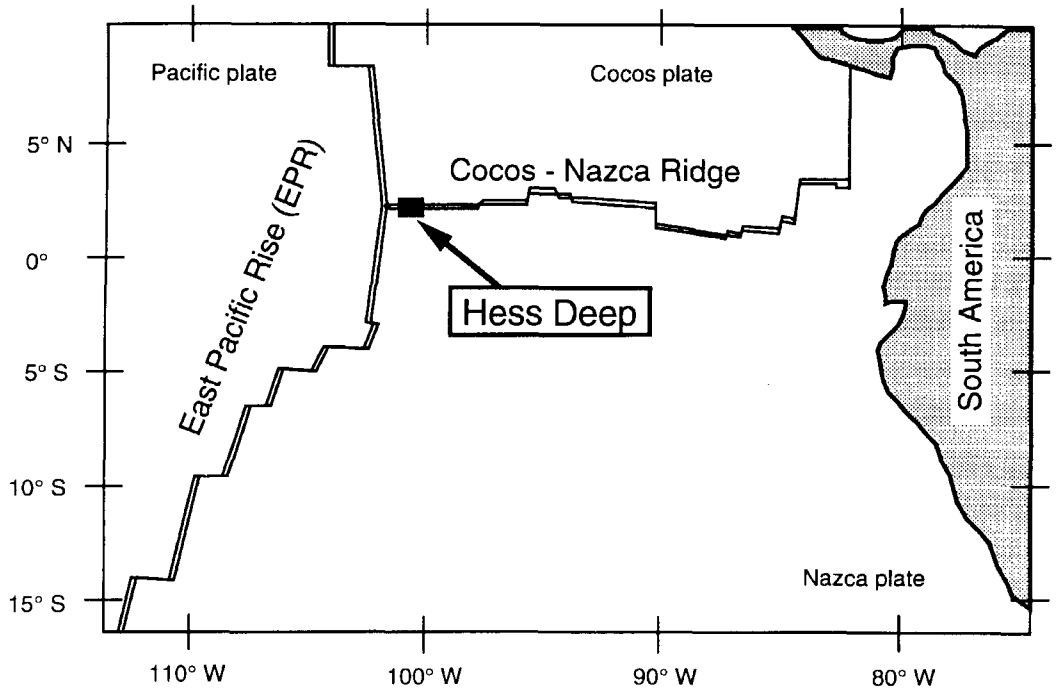

FIG. 1. Location of Hess Deep adjacent to the Pacific-Cocos-Nazca triple junction in the eastern Equatorial Pacific.

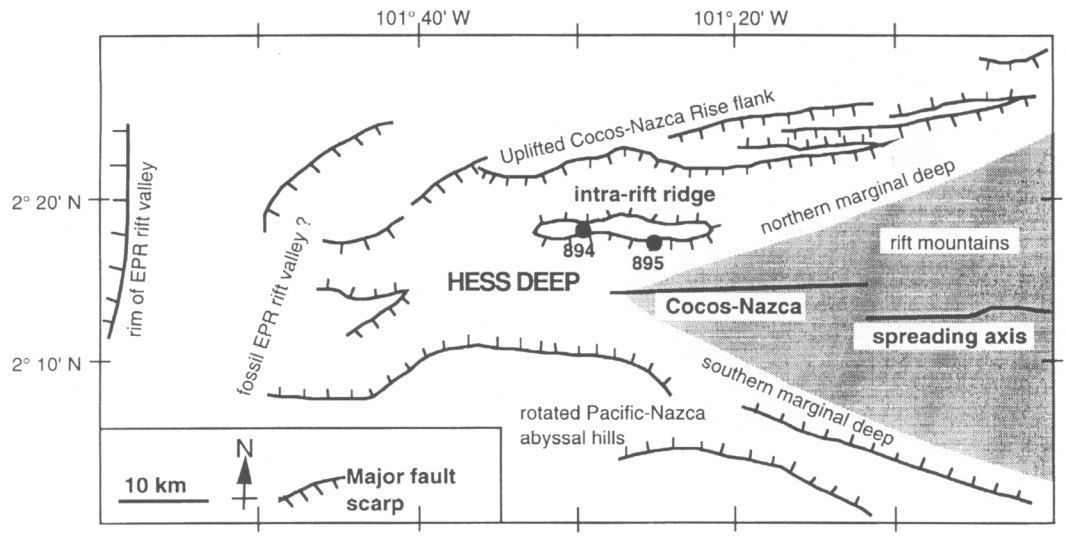

FIG. 2. Location of Hess Deep and ODP Leg 147 Sites 894 and 895 at the western end of the propagating Cocos-Nazca spreading axis; the shaded area represents crust formed at the spreading axis (modified from Lonsdale, 1988).

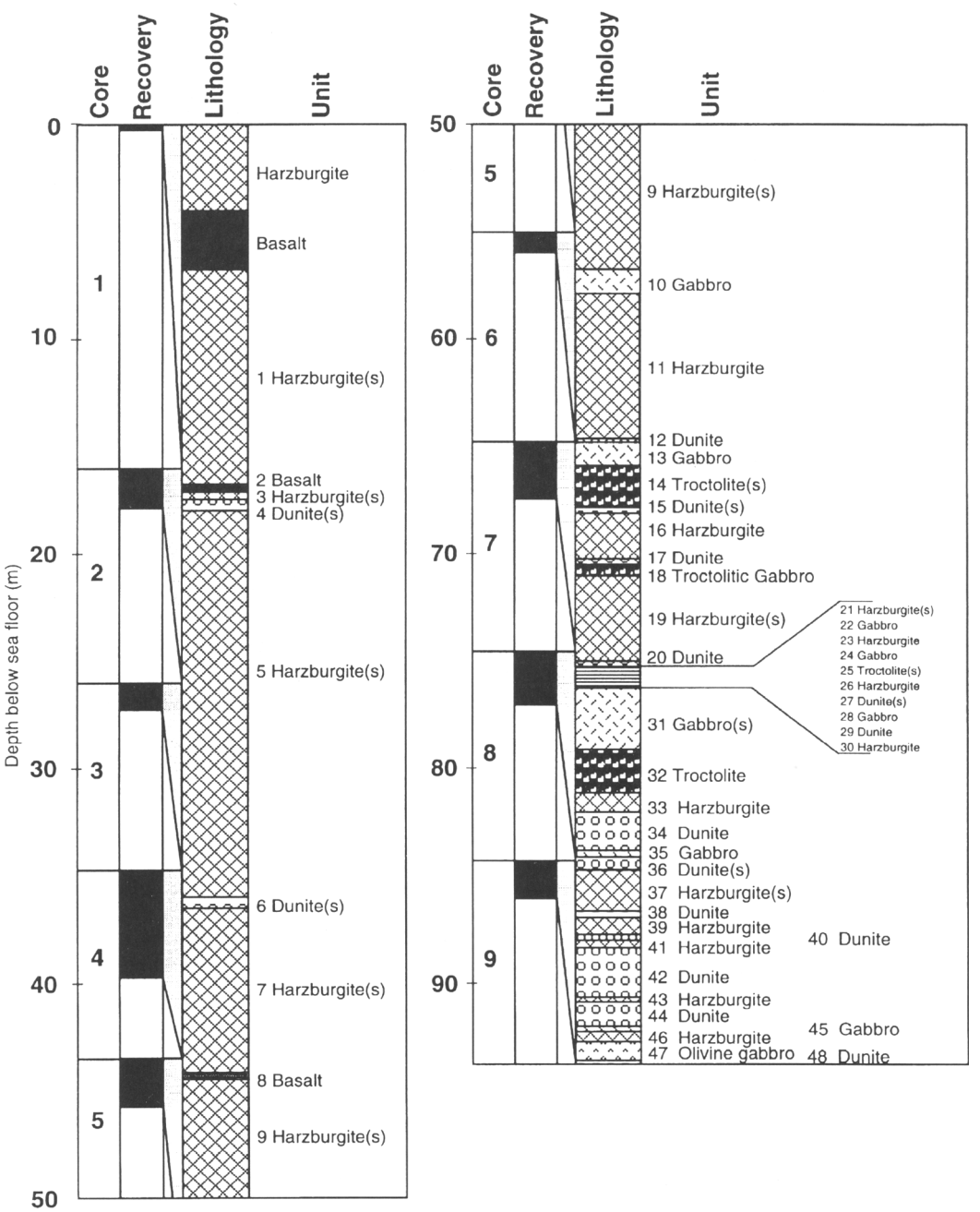

FIG. 3. Schematic lithostratigraphic column for Hole 895D (from Gillis *et al.*, 1993). Units sampled and examined in the present study are denoted by (s) and samples are listed in Appendix I.

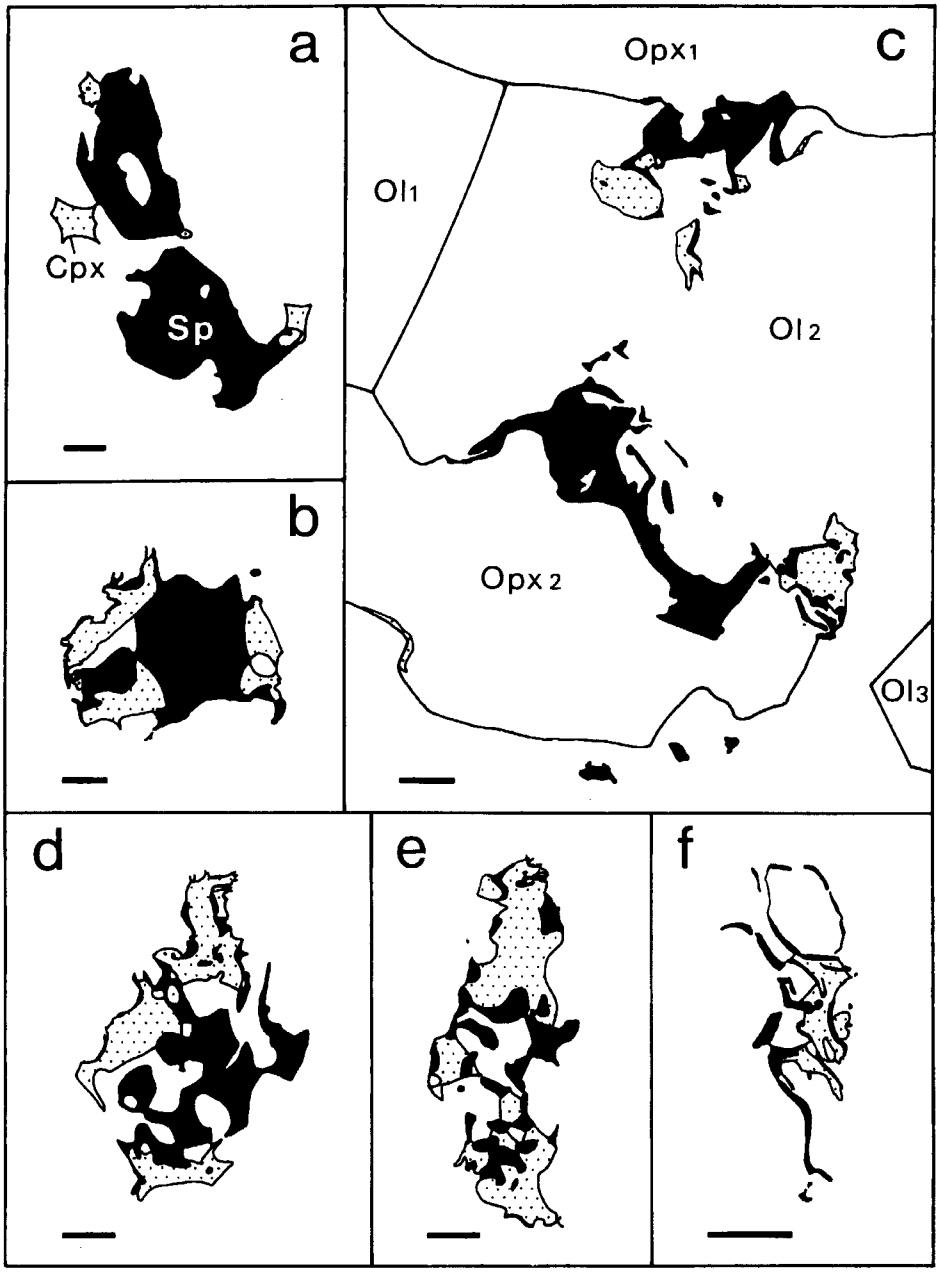

FIG. 4. Line drawings of backscattered electron images of clinopyroxene-spinel associations in variably altered matrices of olivine and orthopyroxene (white) in harzburgite; scale bar represents 100 μm. (*a*) Olivine–orthopyroxene contact: massive, pull-apart, olivine-bearing spinel exhibiting minor new growth of spinel associated with clinopyroxene. (*b*) Completely altered matrix: massive spinel partially overgrown by spinel and clinopyroxene. (*c*) Orthopyroxene porphyroclasts partially replaced by massive grains of olivine and spinel ± clinopyroxene. (*d*) Olivine matrix: poikilitic texture of olivine enclosed in intergrown spinel and clinopyroxene. (*e*) Olivine–orthopyroxene contact: intergrown spinel and clinopyroxene. (*f*) Completely altered olivine-orthopyroxene contact: intricate spinel texture associated with clinopyroxene.

cracks within grains. Despite alteration, metamorphism and subsolidus re-equilibration, original texture, mineralogy and mineral chemistry may be determined from the abundant remnants and pseudomorphs of original grains.

Textural data

Harzburgite. The modal mineralogy of harzburgite is normally 80–90% olivine (but small patches of dunite may exist), 10–20% orthopyroxene, <1% clinopyroxene and ⩽2% spinel (highest abundance in sample 895D-03R-01 (38–43 cm)). The texture of the harzburgite reflects at least two events. A porphyroclastic texture has been severely overprinted by a younger texture formed during melt impregnation and reaction (referred to as an impregnation texture below). The former may still be seen as a high-temperature tectonite fabric which is defined by relatively large porphyroclasts and porphyroclast-neoblast clusters of orthopyroxene, and by porphyroclasts and pulled-apart grains of spinel. No grains of clinopyroxene have been found which correlate with this porphyroclastic texture.

The impregnation texture post-dates deformation and is either new or a modification of the porphyroclastic texture. Olivine exhibits a bimodal grain size, being fine to coarse where it rims and embays orthopyroxene, and coarse away from orthopyroxene. The majority of coarse grains are coarse-granular with well-equilibrated grain boundaries. Clinopyroxene is interstitial with respect to all other phases and locally exhibits poikilitic inclusion of olivine. Very small patches of clinopyroxene may occur in orthopyroxene porphyroclasts. Some may be exsolution lamellae, but the majority are associated with trails of olivine embaying orthopyroxene and with what are assumed to be fractures in orthopyroxene. Almost everywhere, clinopyroxene and spinel occur together.

In harzburgite, porphyroclastic and impregnation textures are best recorded by the morphological variation of spinel and associated silicate minerals. Porphyroclastic and impregnation-related spinel grains occur at olivine-orthopyroxene grain boundaries or within the olivine matrix adjacent to orthopyroxene porphyroclasts. Totally unmodified porphyroclastic spinel textures have not been observed, but remnants of this texture are clearly visible (Fig. 4*a*). The impregnation-related spinel texture is seen as (i) overgrowths of spinel ± clinopyroxene on spinel porphyroclasts (Fig. 4*b*), (ii) growth of spinel ± clinopyroxene along olivine-orthopyroxene grain boundaries where orthopyroxene is partially resorbed (Fig. 4*c*), or (iii) growth of relatively massive and fine grains (Fig. 4*d,e*) or fine grains (Fig. 4*f*), both of which are associated with clinopyroxene.

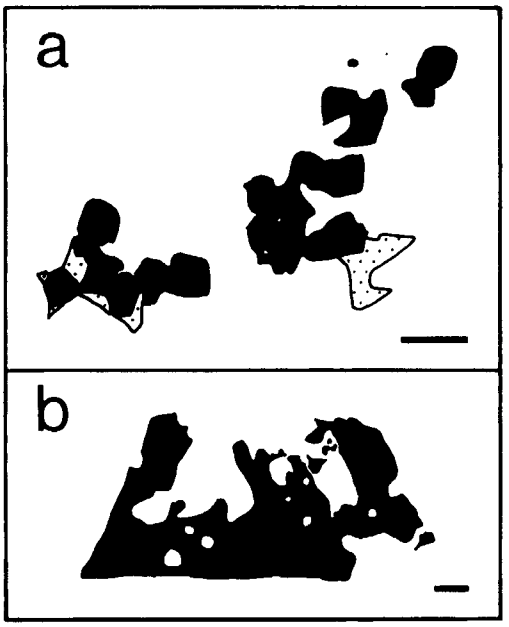

FIG. 5. (*a*) spinel-rich dunite: spinel (black) chain texture with minor interstitial clinopyroxene (dotted) in a completely altered olivine matrix (white); scale bar represents 0.5 mm. (*b*) Troctolite: partially resorbed spinel (black) in plagioclase (white); scale bar represents 100 μm.

Dunite. The modal mineralogy of dunite is normally 96–99% olivine, ⩽3% spinel and traces of clinopyroxene. Olivine is coarse-granular with well-equilibrated grain boundaries. As with all rock types examined from Hole 895D, but most obvious in dunite, olivine contains abundant inclusions. Spinel is an interstitial phase and is rounded, subhedral or euhedral, and may exhibit partial chain texture (Fig. 5*a*). Where present, clinopyroxene is interstitial with respect to olivine and spinel.

In sample 895D-02R-02 (8–12 cm) a contact is preserved between harzburgite and dunite. The contact is sharp and there are no obvious deviations from the features described for the respective rock types and no obvious change in concentration of spinel across the contact.

Gabbroic rocks. Patches and vein networks of gabbroic rock occur throughout the ultramafic host rock (mostly dunite) (Fig. 6). The modal mineralogy of gabbroic rocks is highly variable and may be divided into troctolite and gabbro end-members, which are gradational into one another and their host rock. Troctolites contain 30–90% olivine, 10–70% plagioclase, ⩽5% clinopyroxene and ⩽1% spinel.

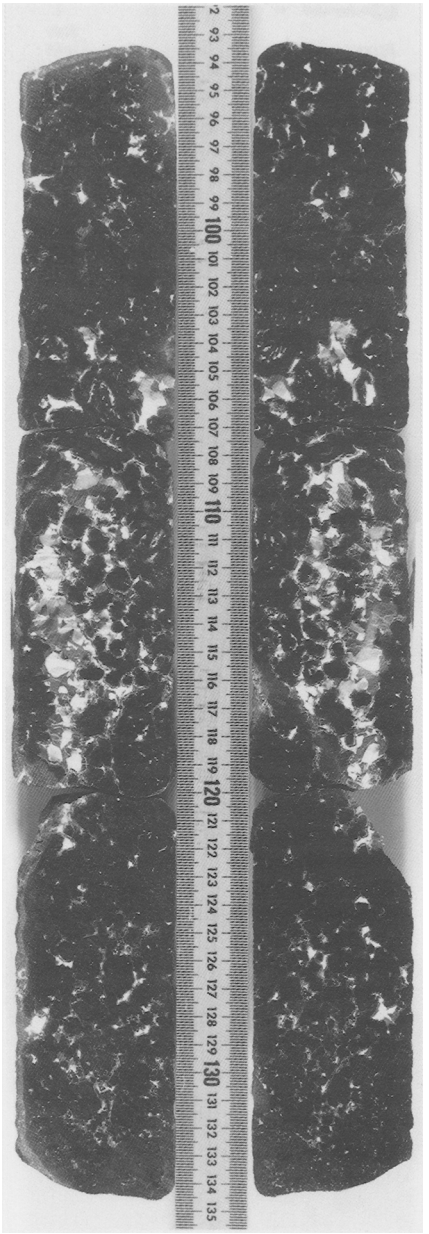

FIG. 6. Photograph of the interval 04R-02 (93–135 cm) in Hole 895C which shows olivine gabbro (plagioclase is white; clinopyroxene is light grey; olivine is black) grading to dunite. The photograph shows that clinopyroxene always lines the contact between plagioclase and olivine, appears before plagioclase where dunite grades into gabbro, and poikilitically encloses plagioclase in gabbro. Hole 895C is only a few metres from Hole 895D.

Spinel is absent in the most plagioclase-rich areas, and generally shows a concomitant increase in abundance with decreasing plagioclase abundance. Wherever spinel occurs, it is always spatially associated with plagioclase and either is irregular in shape, in places partially resorbed and containing silicate inclusions (Fig. 5*b*), or is rounded or subhedral. Gabbros comprise $\leqslant 30\%$ olivine, 40–60% plagioclase, 10–40% clinopyroxene and spinel is absent. Textures in all gabbroic rocks may be described as cumulus. This does not necessarily imply formation through cumulus processes, because these textures may be produced by melt–peridotite interaction (e.g. Nicolas, 1989, and references therein). Relationships between mineral phases do, however, suggest an order of formation: olivine + spinel, plagioclase, clinopyroxene.

Where dunite grades into gabbroic rock, clinopyroxene and plagioclase exhibit a very important relationship as clinopyroxene and then plagioclase become more abundant (Fig. 6): in dunite, clinopyroxene appears before plagioclase and is often intergrown with spinel; when interstitial plagioclase first appears in dunite, it is completely isolated from olivine by a rim of clinopyroxene; in gabbroic patches, plagioclase is separated from olivine by a thin zone of clinopyroxene, and massive grains of clinopyroxene may poikilitically enclose plagioclase. Consequently, this gradation suggests clinopyroxene formed before plagioclase in dunite, but in the adjacent gabbroic rocks the reverse appears to be the case. This relationship and the origin of associated cumulus textures are both extremely important and are discussed later.

Mineral chemistry

Mineral compositions were determined by energy-dispersive and wavelength-dispersive techniques on a Cameca Camebax SX50 electron microprobe at Memorial University of Newfoundland. Standards comprised well-characterised natural minerals and pure metals, and data were reduced using the ZAF correction procedure. Representative mineral analyses are given in Table 1, which should be referred to throughout description of the mineral chemistry. Data for primary silicates are missing for some samples because the relevant phases have been completely altered. Spinel has been analysed in all samples where it occurs.

Olivine. The composition of olivine is apparent from Fig. 7*a*. The Mg# (refer to Table 1 for definition) of olivine in harzburgite ranges from 86.5 to 91.8 (NiO = 0.34–0.46 wt.%). The lower and upper limits of the range are found in harzburgite adjacent to dunite in sample 895D-02R-02 (8–12 cm) and in olivine inclusions in spinel, respectively. In

TABLE 1. Representative mineral analyses

Rock type	Harzburgite	Harzburgite	Harzburgite	Harzburgite	Dunite	Dunite	Dunite	Dunite	Troctolite	Troctolite	Gabbro
Unit	3	19	5	3	4	6	6	27	14	14	31
Core section	02R-01	07R-03	03R-01	02R-02	02R-02	04R-02	04R-02	08R-01	07R-01	07R-01	08R-02
Interval (cm)	038–041	013–016	038–043	008–012	008–012	069–072	069–072	092–097	050–052	086–091	009–012
Olivine											
SiO_2	40.8	41.0	40.8	40.1	40.0	40.7	39.2		40.8	41.0	
FeO	9.1	8.9	8.8	12.7	13.5	9.0	16.5		10.4	10.4	
MnO	0.13	0.16	0.17	0.24	0.22	0.14	1.16		0.19	0.18	
NiO	0.41	0.43	0.37	0.35	0.38	0.41	0.34		0.36	0.34	
MgO	49.3	49.7	49.5	46.2	46.1	49.3	42.5		48.1	48.5	
CaO	bdl	0.07	0.09	0.07	0.21	0.07	bdl		0.08	bdl	
Na_2O	bdl	bdl	0.01	bdl	bdl	0.02	0.02		bdl	bdl	
Total	99.74	100.26	99.74	99.66	100.41	99.64	99.72		99.93	100.42	
Mg#	90.6	90.9	90.9	86.6	85.9	90.7	82.1		89.2	89.3	
Orthopyroxene											
SiO_2	55.6	55.4	55.7	55.5							
TiO_2	bdl	bdl	bdl	0.25							
Al_2O_3	2.2	2.2	2.7	1.8							
Cr_2O_3	0.77	0.79	0.87	0.56							
FeO	5.8	5.2	5.8	8.2							
MnO	0.11	0.10	0.10	0.17							
NiO	0.14	0.10	0.07	0.09							
MgO	33.0	30.5	33.1	31.6							
CaO	1.51	5.7	1.56	1.82							
Na_2O	bdl	bdl	0.03	0.05							
Total	99.09	99.99	99.93	100.04							
Mg#	91.0	91.3	91.0	87.3							
En	88.4	81.3	88.3	84.2							
Fs	8.7	7.8	8.7	12.3							
Wo	2.9	10.9	3.0	3.5							
Clinopyroxene											
SiO_2	52.4	51.8	52.5	52.6	52.0				51.8	51.3	52.3
TiO_2	0.07	bdl	0.05	0.49	0.64				0.73	0.44	0.23
Al_2O_3	2.7	3.1	3.0	2.5	2.7				3.5	3.7	3.1
Cr_2O_3	1.02	1.19	1.38	1.08	1.18				1.21	1.23	1.01
FeO	2.8	2.9	2.6	3.4	3.6				2.9	3.6	3.2
MnO	0.06	0.05	0.07	bdl	0.07				0.07	0.09	0.08
NiO	0.11	0.08	0.04	0.06	bdl				bdl	0.05	bdl
MgO	18.3	18.4	17.2	16.7	16.1				16.8	16.9	16.6
CaO	22.0	22.5	22.8	22.6	22.5				23.5	22.9	22.8
Na_2O	0.02	0.01	0.40	0.74	0.77				0.28	0.24	0.22
Total	99.48	100.03	100.04	100.17	99.56				100.79	100.45	99.54
Mg#	92.1	91.9	92.2	89.7	88.9				91.2	89.3	90.2
En	51.3	50.8	49.1	47.9	47.0				47.6	47.8	47.7
Fs	4.4	4.5	4.2	5.5	5.9				4.6	5.7	5.2
Wo	44.3	44.7	46.8	46.6	47.2				47.8	46.5	47.1
Spinel											
SiO_2	0.11	0.05	0.05	bdl	0.03	0.06		0.11	0.02	0.03	
TiO_2	0.06	0.04	0.08	1.43	1.47	0.04		0.58	0.85	0.98	
V_2O_3	0.26	0.22	0.17	0.55	0.59	0.23		0.26	0.34	0.37	
Al_2O_3	25.7	24.5	30.1	18.8	17.5	25.2		22.3	23.8	21.0	
Cr_2O_3	42.3	43.9	38.7	42.8	39.2	43.8		40.9	39.6	42.9	
FeO	17.2	17.8	15.9	26.6	31.6	16.6		21.3	21.7	22.1	
NiO	0.14	0.15	0.13	0.16	0.27	0.10		0.12	0.16	0.11	
MgO	13.7	13.0	14.3	9.4	8.5	13.6		12.2	11.9	11.3	
ZnO	0.31	0.27	0.32	0.43	0.45	0.27		0.18	0.41	0.27	
Total	99.78	99.93	99.75	100.17	99.61	99.90		97.95	98.78	99.06	
Fe^{2+}	3.0	3.2	2.9	4.6	4.9	3.0		3.5	3.7	3.9	
Fe^{3+}	0.46	0.41	0.26	1.1	1.9	0.32		0.96	0.86	0.77	
Mg#	61.9	59.5	63.6	43.7	40.0	61.8		56.5	54.7	52.2	
Cr#	52.5	54.6	46.3	60.4	60.1	53.8		55.2	52.8	57.8	

Refer to Appendix I for full explanation of rock type, unit and core section. The following compositional parameters are in mol.%: Mg#, 100Mg/(Mg+Fe); Cr#, 100Cr/(Cr+Al); En, 100Mg/(Mg+Fe+Ca); Fs, 100Fe/(Mg+Fe+Ca); Wo, 100Ca/(Mg+Fe+Ca). In silicates Fe is $Fe^{2+}{}_{total}$; in spinel Fe is Fe^{2+} and Fe^{2+} and Fe^{3+} are calculated assuming charge balance and perfect stoichiometry for 32 oxygens and 24 cations. bdl, below 2σ detection limit. K_2O in all silicates is bdl and TiO_2, Al_2O_3 and Cr_2O_3 in olivine are bdl. Generally, the coefficient of variation is <1.6% for >10 wt.% oxide and increases to 3–8% for <3 wt.% oxide.

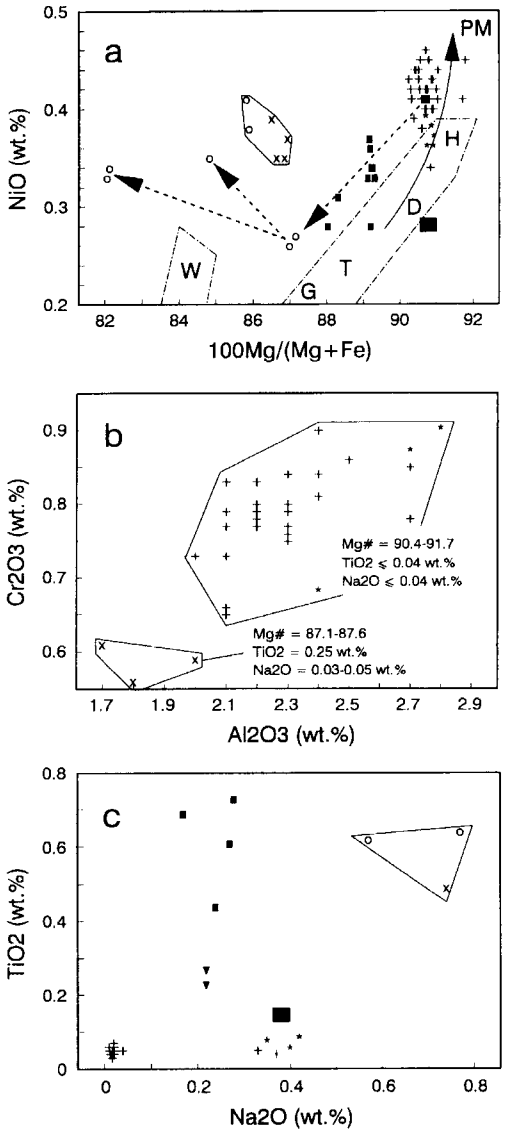

FIG. 7. Compositions of silicate minerals in Hole 895D harzburgite (+), harzburgite adjacent to dunite in sample 895D-02R-02 (8–12 cm) (x), harzburgite sample 895D-03R-01 (38–43 cm) (*), dunite (o), troctolite (solid square) and gabbro (solid inverted triangle); compositions of minerals in harzburgite and dunite in sample 895D-02R-02 (8–12 cm) are encircled. The average compositions of minerals in abyssal spinel peridotites (large solid square) are from Dick and Fisher (1984) (in the case of orthopyroxene Cr_2O_3 = 0.43 wt.% and Al_2O_3 = 4.2 wt.%). (*a*) NiO versus 100Mg/(Mg+Fe) (Mg#) in olivine; dashed arrows connect progressively evolving olivine compositions over a distance of 16 mm in dunite sample 895D-02R-02 (8–12 cm), olivine in dunite adjacent to harzburgite has a composition similar to that in the harzburgite. Olivine in dunite also shows a wide compositional range, the whole of which is observed over a distance of 16 mm in sample 895D-04R-02 (69–72 cm) where Mg# = 82.1–90.7 and NiO = 0.26–0.41 wt.%. In this sample MnO increases from 0.14 to 1.16 wt.% as Mg# decreases, and olivine is so rich in inclusions that it is semi-opaque. Troctolites contain olivine with Mg# = 88.0–89.3 and NiO = 0.28–0.37 wt.% which fall within the compositional range of olivine in dunite.

Orthopyroxene. The composition of orthopyroxene in harzburgite is intermediate between enstatite and bronzite and CaO concentrations are 1.40–5.7 wt.%. The high Ca values reflect the presence of clinopyroxene. There is a positive correlation between Cr and Al concentrations in orthopyroxene (Fig. 7*b*). With respect to all other harzburgites, orthopyroxene in harzburgite adjacent to dunite in sample 895D-02R-02 (8–12 cm) has the lowest Cr and Al concentrations and Mg#s, and highest Ti concentrations (Fig. 7*b*).

Clinopyroxene. The compositional fields of clinopyroxene are best differentiated by TiO_2 and Na_2O (Fig. 7*c*). The majority of harzburgites have clinopyroxene with Mg# = 91.5–93.3, $TiO_2 \leqslant 0.08$ wt.%, and Na_2O of either $\leqslant 0.07$ wt.% or 0.33–0.42 wt.%. Al and Cr concentrations are generally higher in Na-rich clinopyroxenes, and in some samples these concentrations correlate with high Al and Cr in orthopyroxene (e.g. sample 895D-03R-01 (38–43 cm)). Clinopyroxene in harzburgite adjacent to dunite in sample 895D-02R-02 (8–12 cm) is enriched in Fe, Ti and Na, and is compositionally similar to that in the adjacent dunite.

Clinopyroxenes in gabbroic rocks exhibit a wide range of Ti concentrations for a restricted range of Na concentrations and the highest Ti values occur in troctolite. Of all the rock types, gabbroic rocks have clinopyroxenes with the highest Al concentrations.

Plagioclase. The anorthite content of plagioclase in troctolites is 86.2-87.3 and all analysed grains are devoid of K.

sample 895D-04R-02 (69–72 cm). Progressive partial melting trend (PM) is from Girardeau and Francheteau (1993) and dash-dot lines enclose Hess Deep olivine compositions reported by Hekinian *et al.* (1993): harzburgite and melt-impregnated harzburgite (H), harzburgite impregnated by wehrlite (W), dunite (D), troctolite (T), olivine gabbro and olivine gabbro/troctolite (G). (*b*) Cr_2O_3 versus Al_2O_3 in orthopyroxene in harzburgite; values for Mg# and Ti content demonstrate wide variation in orthopyroxene composition. (*c*) TiO_2 versus Na_2O in clinopyroxene.

Spinel. All spinels analysed in harzburgite, dunite and troctolite are Cr-rich with Cr_2O_3 = 37.9–44.1 wt.%. Within a given sample, the composition of grain interiors is remarkably similar regardless of grain size or texture. Figure 8 shows that spinel exhibits significant variation in Mg#, Cr#, Ti content and Fe^{2+}/Fe^{3+} ratio (refer to Table 1 for definition of Mg#, Cr#, Fe^{2+} and Fe^{3+}). The highest Mg#s and lowest Cr#s are restricted to harzburgites in which orthopyroxene has the highest concentrations of Cr and Al and clinopyroxene has high concentrations of Na, Al and Cr, which is best exemplified by sample 895D-03R-01 (38–43 cm). With respect to this spinel composition, spinels in the majority of harzburgites have similar or lower Mg#s, higher Cr#s, and the same Ti concentrations. Dunite sample 895D-04R-02 (69–72 cm) contains olivine with Mg# = 82.1–90.7 and spinel associated with olivine of highest Mg# has a composition identical to that of the main group of harzburgites with Ti-depleted spinels. With decreasing Mg# and increasing Cr#, these spinel compositions overlap with those in troctolite and dunitic zones between harzburgite and gabbroic rocks, but spinel in these dunites and troctolites are enriched in Ti. The lowest Mg#s and highest Cr#s and Ti concentrations in spinel are found in harzburgite and dunite in sample 895D-02R-02 (8–12 cm).

Spinels in all rock types, when considered together, follow a general trend of decreasing Fe^{2+}/Fe^{3+} ratio as total Fe increases and Mg# decreases, and as Al decreases and Cr# increases (Fig. 8*a,c*). The most oxidised spinel occurs in dunite adjacent to harzburgite in sample 895D-02R-02 (8–12 cm), and the least oxidised includes spinel in harzburgite sample 895D-03R-01 (38–43 cm). With the samples studied, there does not appear to be a systematic correlation of this trend with the degree of alteration of the rock hosting spinel, despite dunites with spinel with the lowest Fe^{2+}/Fe^{3+} ratio being amongst the most extensively altered samples. Although spinel in dunite defines a trend of increasing Cr# with decreasing Mg# (Fig. 8*a*), which may be produced by alteration (Bliss and MacLean, 1975; Jan and Windley, 1990), spinel in the most altered harzburgite sample exhibits the opposite trend and plots with spinels in sample 895D-03R-01 (38-43 cm) (Fig. 8*a*). As will be discussed later, the compositional trends exhibited by spinel in dunite may be adequately explained by magmatic processes.

Comparison with other studies. The compositions of minerals in the ultramafic and mafic rocks analysed from Hole 895D are expected for these rock types formed in an oceanic environment. The compositions and compositional evolutionary trends of olivine and spinel are similar to those previously reported for Hess Deep samples by Hekinian *et al.* (1993), with olivine in Hole 895D having a higher Ni content (Figs. 7*a* and 8*a*). With the exception of sample 895D-02R-02 (8–12 cm), spinel in Hole

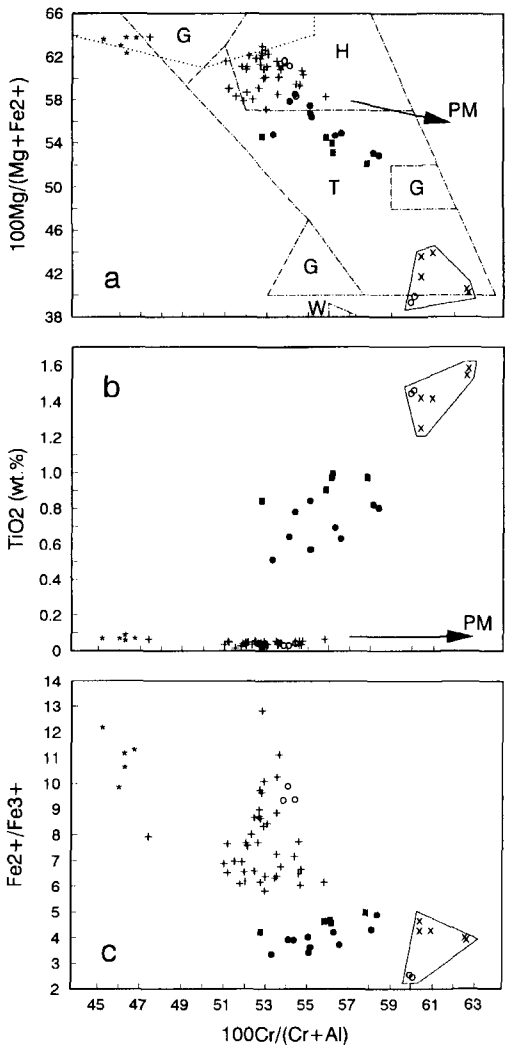

FIG. 8. Spinel compositions in Hole 895D rock types. Symbols and letters as in Fig. 7, except solid circles represent spinel in dunite adjacent to gabbroic rocks, and the progressive partial melting trend (PM) in (*a*) is from Dick and Bullen (1984) and in (*b*) is from Girardeau and Francheteau (1993). (*a*) 100Mg/(Mg+Fe^{2+}) (Mg#) versus 100Cr/(Cr+Al) (Cr#); dotted lines enclose the field occupied by Cr-rich spinel in abyssal spinel peridotites (Dick and Fisher, 1984). (*b*) TiO_2 versus 100Cr/(Cr+Al). (*c*) Fe^{2+}/Fe^{3+} versus 100Cr/(Cr+Al).

895D harzburgites plots at the Cr-rich end of the field defined by spinel in abyssal spinel peridotites (Fig. 8*a*). Figure 7 shows that silicates in the majority of Hole 895D harzburgites are much more refractory than those in an average abyssal peridotite. As far as we know, the high concentrations of Na, with and without high concentrations of Ti, have not previously been documented for clinopyroxene in harzburgites formed at the EPR and sampled at Hess Deep (Girardeau and Francheteau, 1993; Hekinian *et al.*, 1993) or Garrett Deep (Hébert *et al.*, 1983; Cannat *et al.*, 1990). Hole 895D gabbroic rocks occupy the high forsterite-high anorthite region of the MORB field illustrated by Browning (1984).

Harzburgite: textural development and mineral chemical evolution

The texture, mineralogy and mineral chemistry of Hole 895D harzburgite suggests a complex two-stage evolution through partial melting and later melt–harzburgite interaction. With the exception of sample 895D-02R-02 (8–12 cm), the refractory mineral compositions could be expected to result solely from partial melting. The texture of orthopyroxene porphyroclasts and neoblasts and spinel porphyroclasts supports such an origin by partial melting before or during asthenospheric (>1000°C) flow. However, the impregnation texture of resorbed orthopyroxene and growth and recrystallisation of olivine and spinel, in most cases associated with undeformed, interstitial clinopyroxene, resulted from melt–harzburgite interaction after asthenospheric deformation. Not only did this interaction affect the porphyroclastic texture and residual mineralogy, it is believed to have modified the residual mineral chemistry. Reactions (1), (2) and (3) describe the most important mineralogical changes which probably occurred simultaneously during melt–harzburgite interaction.

$$Mg_2Si_2O_6 \text{ (peridotite)} + \text{melt} \rightarrow Mg_2SiO_4 \text{ (peridotite)} + SiO_2 \text{ (melt)} \quad (1)$$

$$Mg_2Si_2O_6 \text{ (peridotite)} + CaAl_2Si_2O_8 \text{ (melt)} \rightarrow CaMgSi_2O_6 \text{ (peridotite)} + MgAl_2O_4 \text{ (peridotite)} + 2SiO_2 \text{ (melt)} \quad (2)$$

$$Mg_2SiO_4 \text{ (peridotite)} + CaAl_2Si_2O_8 \text{ (melt)} \rightarrow CaMgSi_2O_6 \text{ (peridotite)} + MgAl_2O_4 \text{ (peridotite)} + SiO_2 \text{ (melt)} \quad (3)$$

The abundance of olivine in harzburgite would have increased during reaction, due to the incongruent breakdown of orthopyroxene (reaction 1) and, possibly, by direct crystallisation from the melt, with the eventual formation of dunite. The coarse granular grains of olivine now present may have formed from pre-existing fine, deformed grains and/or newly formed grains through recrystallisation at around 1300°C in the presence of melt (Nicolas, 1986). Such temperatures may have been reached during melt migration through Hess Deep harzburgite, as equilibration of clinopyroxene impregnations has been estimated at 1045–1151°C at <6 km by Hekinian *et al.* (1993).

Reactions (2) and (3) explain the close association of clinopyroxene and spinel and absence of plagioclase, as a result of the latter, a liquidus phase or previous crystallisation product, reacting with the peridotite matrix. According to the classification of spinel structures by Suhr (1991), the majority of spinel textures in Hole 895D harzburgites correspond with textural re-equilibration and new growth during melt flushing and melt impregnation, with the latter process being dominant.

The textures which developed in all harzburgites during melt interaction were similar, whereas the mineral compositions were significantly variable. With respect to the majority of harzburgite samples, two obvious melt–interaction trends are definable, in which enrichment is defined with respect to compositions of olivine, orthopyroxene and spinel. The first resulted from Fe-Ti enrichment and is exemplified by harzburgite adjacent to dunite in sample 895D-02R-02 (8–12 cm), in which olivine has a relatively low Ni content and is enriched in Fe, orthopyroxene is enriched in Fe and Ti and depleted in Al and Cr, and clinopyroxene is relatively rich in Fe, Ti and Na (Table 1 and Fig. 7). Spinel is depleted in Al and Mg and enriched in Ti, V and Fe; the low Fe^{2+}/Fe^{3+} ratio contributes to the high Cr# (Table 1 and Fig. 8). This trend is similar to Fe-Ti enrichment and Al depletion in melt-impregnated harzburgites examined from Hess Deep by Hekinian *et al.* (1993) and from Garrett Deep by Cannat *et al.* (1990).

The second trend reflects Al enrichment and is most pronounced in the harzburgite sample richest in spinel, sample 895D-03R-01 (38–43 cm), in which olivine is depleted in Ni for a given Mg#, orthopyroxene may show a slight enrichment in Al and Cr, clinopyroxene shows a slight decrease in Mg# and is relatively rich in Al, Cr and Na, and spinel is enriched in Al and depleted in V and Cr (Table 1 and Figs. 7 and 8). This trend for spinel corresponds with the Al-enrichment trend followed by spinels in the Rhum layered intrusion, where enrichment also resulted from reaction between Cr-spinel, olivine and plagioclase (Henderson, 1975).

In all samples where residual minerals exhibit enrichment of one kind or another, the fact that the cores of mineral grains are enriched implies either that the minerals completely recrystallised in the presence of melt, or that diffusion within grains was pervasive. The latter is particularly relevant to

orthopyroxene, which must have exchanged elements by diffusion at the same time as grain margins were being resorbed. Hence, the compositions of residual minerals reflect chemical re-equilibration with migrating melt. The implication of this is discussed later.

Origin of dunite and gabbroic rocks

Dunite and gabbroic rocks are closely associated in Hole 895D and harzburgite may grade into a gabbroic rock through an intermediate of dunite (Figs. 3 and 6). This is unlikely to be coincidental and rules out an origin of dunite through partial melting, as it would be more abundant in harzburgite and contain spinel with Cr#>80 (Jaques and Green, 1980). In addition, dunite and gabbroic rocks at Site 895 have been found to contain partially digested porphyroclasts of orthopyroxene (Gillis *et al.*, 1993). Hence, dunite and associated gabbroic rocks are believed to be products of melt–harzburgite interaction and are best considered in terms of reaction (4):

$$Ol_H + Opx_H + Sp_H + \text{melt} \rightarrow Ol_H + Ol_R + Ol_C + Sp_H + Sp_R + Sp_C + Cpx_R + Cpx_C + Opx_H \text{ (low m/p)} + Plag_C \text{ (high m/p)} \quad (4)$$

where H is harzburgite, R is a reaction product, C is a product crystallised directly from melt, and m/p is the melt/peridotite ratio. The proportion of each mineral depends principally on the starting compositions of the reacting harzburgite and melt, the melt/peridotite ratio, and the nature and extent of melt–harzburgite interaction.

As recorded in harzburgite, the first step in reaction at low melt/peridotite ratio involved partial or complete incongruent dissolution of orthopyroxene and formation of olivine and minor spinel ± clinopyroxene (reactions 1–3). With further reaction and crystallisation, as melt disaggregated the olivine matrix (relatively high melt/peridotite ratio), olivine-bearing and olivine-free gabbroic rocks formed, respectively. Between these two extremes, dunite may be formed; this is exemplified by the occurrence of dunite between harzburgite and gabbroic rocks in Hole 895D (Fig. 3). Through crystallisation and recrystallisation of mineral phases, dunites and gabbroic rocks developed textures which mimic those of cumulates (Violette, 1980; Nicolas and Prinzhofer, 1983; Edwards, 1991), despite plagioclase being the only phase which originated solely by crystallisation directly from melt (reaction 4).

The wide range of mineral compositions found in dunites is expected to arise from melt–peridotite interaction. In dunite sample 895D-04R-02 (69–72 cm), the change in Mg# of olivine from 82.1 to 90.7 over a distance of 16 mm suggests chemical re-equilibration of olivine which is controlled by the composition of melt and harzburgite, respectively. The abundance of inclusions in olivine in this sample implies recrystallisation occurred during melt flushing. In sample 895D-02R-02 (8–12 cm), the similarity of relatively evolved mineral compositions in harzburgite and dunite indicates that in harzburgite chemical modification preceded, or was contemporaneous with, textural and mineralogical modification, and this appears to have required both intergrain and intragrain diffusion.

The possible genetic relationship between dunite and gabbroic rocks may explain the similarity of mineral compositions in their residual and melt components. A case in point is the composition of spinel in Fig. 8. Spinels in troctolites and dunites associated with gabbroic rocks have very similar compositions. This, and the fact that their Mg#-Cr# variation (Fig. 8*a*) defines a trend similar to the olivine-plagioclase control line in the diagrams of Leblanc and Violette (1983) and Dick and Bullen (1984), suggests that spinel compositions in these rocks are controlled by the presence of plagioclase in troctolite and in gabbroic rocks adjacent to dunite. The removal of the $MgAl_2O_4$ component from spinel may have resulted during leaching by melt with plagioclase on the liquidus, or by subsolidus re-equilibration controlled by plagioclase (cf. Irvine, 1967; Henderson, 1975). The leaching process is supported by partially resorbed spinel grains in troctolite (Fig. 5*b*). In this case, the effect of a high melt/peridotite ratio (represented by gabbroic zones and patches) on controlling the composition of spinel in dunite formed by replacement of harzburgite, suggests that spinel in the olivine matrix was able to exchange elements with melt either by diffusion through olivine or by direct contact with melt along grain boundaries and fractures. These types of exchange reactions have been well documented in the Jimberlana intrusion by Roeder and Campbell (1985). The melt(s) responsible for these chemical changes in spinel is predicted to have been somewhat evolved because of the Ti and Fe^{3+} content of spinel, which would also explain why the spinels plot on an olivine-plagioclase control line. At this stage, speculation suggests that the mineral compositions in sample 895D-02R-02 (8–12 cm) may in some way also reflect olivine–plagioclase control involving a more evolved melt than that which was involved in the formation of troctolites and dunites associated with gabbroic rocks.

Discussion

In accordance with studies of melt–peridotite interactions and the mantle–crust boundary in ophiolites (e.g. Nicolas and Prinzhofer, 1983; Evans, 1985; Evans and Hawkins, 1989; Nicolas, 1989; Suhr

and Robinson, 1994), the wide variation in texture, mineralogy and mineral chemistry of ultramafic and mafic rock types in Hole 895D is typical of the mantle–crust transition zone, where fractionating basaltic melt(s) has migrated through and interacted with refractory mantle peridotites (reactions 1–4). In this zone, the mechanism of melt migration and the melt/peridotite ratio are both extremely important in controlling melt crystallisation and/or reaction, and mantle refertilization.

Melt migration

Below the transition zone, melt may migrate dominantly by dyke propagation resulting from hydraulic fracturing of peridotite, but this mechanism is difficult to sustain at the transition zone and melt is dispersed into the peridotite matrix (Nicolas, 1989). If this melt is capable of reacting with peridotite, then chemical-driven migration may become extremely important (Watson, 1982; Edwards, 1991). Hence, the transition zone may be a region where there is a significant change from dominantly physical-driven melt migration below, to physical-driven and chemical-driven melt migration in the zone itself. If true, this may explain why melt–peridotite interaction culminates at the transition zone and alters the texture, mineralogy and mineral chemistry of a significant volume of mantle peridotite. However, more work is needed on this subject, particularly in view of the model of focused porous melt flow proposed by Kelemen *et al.* (1995).

Melt crystallisation versus reaction

At low pressure (<9–10 kbar), the crystallisation sequence of MORBs is olivine + spinel, olivine + spinel + plagioclase, olivine + spinel + plagioclase + clinopyroxene, olivine + spinel + plagioclase + clinopyroxene + orthopyroxene (Shido *et al.*, 1971; Shibata, 1976). In the present study, the most significant aspect of this sequence is the appearance of plagioclase before clinopyroxene, particularly because olivine and spinel have multiple origins in many of the mafic and ultramafic rocks (reactions 1–4). The gabbroic rocks from Hole 895D comply with the low-pressure MORB crystallisation sequence, as plagioclase appears before clinopyroxene. As the impregnated melt in harzburgite and dunite appears to be related to that from which the gabbroic rocks formed, it should have crystallised plagioclase before clinopyroxene. However, the impregnated melt component in these peridotites is represented by clinopyroxene ± spinel (Fig. 4), and plagioclase has only been identified in dunite adjacent to gabbroic rocks (Fig. 6). This may be explained by refractory harzburgites resorbing the plagioclase component of impregnating melt (reactions 2 and 3), because these peridotites are highly undersaturated with respect to plagioclase (Jaques and Green, 1980; Kelemen, 1990). Hence, at low melt/peridotite ratio (harzburgite and most dunite) clinopyroxene ± spinel form to the complete exclusion of plagioclase; at high ratios (gabbroic rocks) plagioclase forms before clinopyroxene (reaction 4). At these high ratios, clinopyroxene forms along the reactive interface (Fig. 6). Once formed, this clinopyroxene inhibits further reaction by acting as a barrier between the reacting components. Eventually, melt migrates through and/or collects in regions where clinopyroxene has sealed off the reacting components. At this stage (highest melt/peridotite ratio), normal fractional crystallisation takes place and plagioclase crystallises before clinopyroxene.

The effect of melt/peridotite ratio is not only seen in texture and mineralogy, but also in mineral chemistry. At low melt/peridotite ratios, the plagioclase component of the melt was completely consumed in the formation of clinopyroxene ± spinel, which explains the highest abundance of spinel in harzburgite exhibiting the most extensive Al enrichment in ferromagnesian minerals (sample 895D-03R-01 (38–43 cm)). This enrichment was controlled by the melt because harzburgite originally was highly depleted in these elements. There is no associated change in Mg# of silicates because at low melt/peridotite ratio the highly refractory composition of harzburgite buffered the Mg-Fe composition of the melt–harzburgite system. This does not preclude the possibility that prior to interaction the Mg-Fe composition of the melt was in equilibrium with that of harzburgite.

The origin of Fe-Ti enrichment in minerals in harzburgite has already been discussed in conjunction with the origin of dunite and gabbroic rocks.

Refertilization of upper sub-oceanic mantle

Elthon (1992) has proposed that abyssal peridotites are refertilized when basaltic melt migrates through upper (<5 kbar) sub-oceanic mantle. The evidence for this process comes principally from whole-rock variations in major and minor elements, which suggest addition of 10% depleted basaltic melt to residual peridotite (Elthon, 1992). Obviously this refertilization should be reflected in the texture, mineralogy and mineral chemistry of the peridotites involved.

All interstitial clinopyroxene examined in Hole 895D harzburgite has here been attributed to melt–harzburgite interaction. Also, in the majority of cases, the presence of clinopyroxene, and high Ca values, in orthopyroxene may be attributed to melt

impregnation and reaction. In support of this, Hekinian *et al.* (1993) suggested that the compositional similarity of clinopyroxene in melt impregnations and in exsolution lamellae in orthopyroxene in Hess Deep harzburgites reflects partial re-equilibration between orthopyroxene and melt. The majority of evidence, therefore, implies that prior to the impregnation event, harzburgite formed by melting of mantle to, or beyond the clinopyroxene-out phase boundary, which is beyond the limit normally expected beneath mid-ocean ridges (Dick and Bullen, 1984; Dick and Fisher, 1984). In this situation the Cr# of spinel should have been >55 (Dick and Bullen, 1984). Ignoring sample 895D-02R-02 (8–12 cm), all spinels have Cr#<56 and the Al content of orthopyroxene is much lower than expected for these Cr#s when compared with the compositions of abyssal orthopyroxenes reported by Dick and Fisher (1984). This Al content of orthopyroxene, and the predicted absence of a high diopside component in orthopyroxene prior to melt impregnation, requires that spinel in harzburgite must have been more refractory before melt impregnation. Some evidence for this is provided by higher Cr#s reported by Hekinian *et al.* (1993) for spinel in Hess Deep harzburgite and melt-impregnated harzburgite (Fig. 8*a*). Hence, the progressive partial melting trends defined by spinel in Hole 895D harzburgite (Fig. 8*a,b*) are unlikely to have resulted from partial melting, but from refertilization of harzburgite which was more refractory than that sampled in Hole 895D. The progressive partial melting trend defined by olivine in Fig. 7*a* also is consistent with refertilization. Thus, during refertilization, whereby harzburgite resorbed a basaltic component which had previously been removed from it, new minerals formed and new and residual mineral compositions evolved in the direction opposite to that expected to result from partial melting. This is seen as dissolution of, and Al enrichment in, orthopyroxene, formation of clinopyroxene with variable concentrations of Na, and increase in the abundance of, and $MgAl_2O_4$ enrichment in, spinel.

Refertilization of residual mantle is likely to be most pronounced at the mantle–crust transition zone, as it is here that melt is dispersed into the peridotite matrix. At low melt/peridotite ratios, refertilization will occur without the appearance of plagioclase (Al enrichment trend associated with formation of clinopyroxene ± spinel) and Mg#s of all phases will be buffered by harzburgite. However, as this ratio increases, plagioclase will appear and become progressively more abundant and eventually gabbroic rocks will form. In this case, all mineral compositions are largely buffered by the composition of the melt (Fe-Ti enrichment). Therefore, whereas lherzolite, harzburgite and dunite, respectively, are produced by progressive partial melting, refertilization of refractory harzburgite at low pressure, with increasing melt/peridotite ratio, will progressively produce clinopyroxene-bearing harzburgite (with spinel concentration increasing with Al enrichment), clinopyroxene-bearing dunite and, finally, olivine–clinopyroxene–plagioclase assemblages which eventually become gabbroic. In turn, this suggests that a wide range of melt compositions may be produced from a relatively uniform melt composition which has been changed as a result of reaction over a range of melt/peridotite ratios. Studies are underway to investigate this aspect of melt evolution.

Acknowledgements

C. Emerson, P. King, M. Piranian and D. Williams (Memorial University) and K. Hudson-Edwards and S. Caldwell (Manchester University) assisted with scanning electron microscopy, mineral analysis and photography. D. Groom (Manchester Metropolitan University) helped with drafting. The Department of Earth Sciences at Manchester University is thanked for making available their scanning electron microscope. M. Henderson and M. Hole provided thoughtful and constructive reviews on an earlier version of the manuscript. J. Malpas participated in ODP Leg 147 and this study was supported by a Natural Sciences and Engineering Research Council of Canada Collaborative Special Project Grant to J. Malpas and departmental research funds to S. Edwards.

Note: complete lists of mineral analyses are available on request from S. Edwards.

References

Bliss, N.W. and MacLean, W.H. (1975) The paragenesis of zoned chromite from central Manitoba. *Geochim. Cosmochim. Acta*, **39**, 973–90.

Browning, P. (1984) Cryptic variation within the cumulate sequence of the Oman ophiolite: magma chamber depth and petrological implications. In *Ophiolites and Oceanic Lithosphere* (I.G. Gass, S.J. Lippard and A.W. Shelton, eds.). *Geol. Soc. Lond. Spec. Publ.*, **13**, 71–82.

Cannat, M., Bideau, D. and Hébert, R. (1990) Plastic deformation and magmatic impregnation in serpentinized ultramafic rocks from the Garrett transform fault (East Pacific Rise). *Earth Planet. Sci. Lett.*, **101**, 216–32.

Dick, H.J.B. and Bullen, T. (1984) Chromian spinel as a petrogenetic indicator in abyssal and alpine-type peridotites and spatially associated lavas. *Contrib Mineral. Petrol.*, **86**, 54–76.

Dick, H.J.B. and Fisher, R.L. (1984) Mineralogic studies of residues of mantle melting: abyssal and alpine-

type peridotites. In *Kimberlites II: the Mantle and Crust-Mantle Relationships* (J. Kornprobst, ed.). Elsevier, Amsterdam, 295–308.

Dick, H.J.B., Natland. J. and Leg 147 Scientific Party (1994) Melt transport and evolution in the shallow mantle beneath the East Pacific Rise: preliminary results from ODP Site 895. *Abstracts, Goldschmidt Conference, Edinburgh, Mineral. Mag.*, **58A**, 229–30.

Duncan, R.A. and Green, D.H. (1987) The genesis of refractory melts in the formation of oceanic crust. *Contrib. Mineral. Petrol.*, **96**, 326–42.

Edwards, S.J. (1991) *Magmatic and fluid processes in the upper mantle: a study of the Bay of Islands Ophiolite Complex, Newfoundland.* Unpubl. Ph.D. thesis, Memorial University of Newfoundland, Canada.

Elthon, D. (1992) Chemical trends in abyssal peridotites: refertilization of depleted suboceanic mantle. *J. Geophys. Res.*, **97**, 9015–25.

Evans, C.A. (1985) Magmatic 'metasomatism' in peridotites from the Zambales ophiolite. *Geology*, **13**, 166–9.

Evans, C.A. and Hawkins, J.W., Jr. (1989) Compositional heterogeneities in upper mantle peridotites from the Zambales Range ophiolite, Luzon, Philippines. *Tectonophys.*, **168**, 23–41.

Fisk, M.R. (1986) Basalt-magma interactions with harzburgite and the formation of high magnesium andesites. *Geophys. Res. Lett.*, **13**, 467–70.

Francheteau, J., Armijo, R., Cheminée, J.L., Hekinian, R., Lonsdale, P. and Blum, N. (1990) 1 Ma East Pacific Rise oceanic crust and uppermost mantle exposed by rifting in Hess Deep (Equatorial Pacific Ocean). *Earth Planet. Sci. Lett.*, **101**, 281–95.

Gillis, K., Mével, C., Allan, J., *et al.* (1993) *Proceedings of the Ocean Drilling Program, Initial Reports, 147.* College Station, Texas (Ocean Drilling Program).

Girardeau, J. and Francheteau, J. (1993) Plagioclase-wehrlites and peridotites on the East Pacific Rise (Hess Deep) and the Mid-Atlantic Ridge (DSDP Site 334): evidence for magma percolation in the oceanic upper mantle. *Earth Planet. Sci. Lett.*, **115**, 137–49.

Hébert, R., Bideau, D. and Hekinian, R. (1983) Ultramafic and mafic rocks from the Garrett transform fault near 13°30′S on the East Pacific Rise: igneous petrology. *Earth Planet. Sci. Lett.*, **65**, 107–25.

Hekinian, R., Bideau, D., Francheteau, J., Cheminée, J.L., Armijo, R., Lonsdale, P. and Blum, N. (1993) Petrology of the East Pacific Rise crust and upper mantle exposed in Hess Deep (eastern Equatorial Pacific). *J. Geophys. Res.*, **98**, 8069–94.

Henderson, P. (1975) Reaction trends shown by chrome-spinels of the Rhum layered intrusion. *Geochim. Cosmochim. Acta*, **39**, 1035–44.

Irvine, T.N. (1967) Chromian spinel as a petrogenetic indicator. Part 2. Petrologic applications. *Can. J. Earth Sci.*, **4**, 71–103.

Jan, M.Q. and Windley, B.F. (1990) Chromian spinel-silicate chemistry in ultramafic rocks of the Jijal Complex, northwest Pakistan. *J. Petrol.*, **31**, 667–715.

Jaques, A.L. and Green, D.H. (1980) Anhydrous melting of peridotite at 0–15 kb pressure and the genesis of tholeiitic basalts. *Contrib. Mineral. Petrol.*, **73**, 287–310.

Kelemen, P.B. (1990) Reaction between ultramafic rock and fractionating basaltic magma I. Phase relations, the origin of calc-alkaline magma series, and the formation of discordant dunite. *J. Petrol.*, **31**, 51–98.

Kelemen, P.B., Joyce, D.B., Webster, J.D. and Holloway, J.R. (1990) Reaction between ultramafic rock and fractionating basaltic magma II. Experimental investigation of reaction between olivine tholeiite and harzburgite at 1150–1050°C and 5 kb. *J. Petrol.*, **31**, 99–134.

Kelemen, P.B., Dick, H.J.B. and Quick, J.E. (1992) Formation of harzburgite by pervasive melt/rock reaction in the upper mantle. *Nature*, **358**, 635–41.

Kelemen, P.B., Whitehead, J.A., Aharonov, E. and Jordahl, K.A. (1995) Experiments on flow focusing in soluble porous media, with applications to melt extraction from the mantle. *J. Geophys. Res.*, **100**, 475–96.

Leblanc, M. and Violette, J.-F. (1983) Distribution of aluminum-rich and chromium-rich chromite pods in ophiolite peridotites. *Econ. Geol.*, **78**, 293–301.

Leblanc, M., Dupuy, C., Cassard, D., Moutte, J., Nicolas, A., Prinzhoffer, A., Rabinovitch, M. and Routhier, P. (1980) Essai sur la génèse des corps podiformes de chromitite dans les péridotites ophiolitiques: étude des chromites de Nouvelle-Calédonie et comparaison avec celles de Méditerranée orientale. In *Ophiolites. Proceedings of the International Ophiolite Symposium, Cyprus 1979* (A. Panayiotou, ed.). Geol. Surv. Cyprus, Nicosia, 691–701.

Lonsdale, P. (1988) Structural pattern of the Galapagos microplate and evolution of the Galapagos triple junction. *J. Geophys. Res.*, **93**, 13551–74.

Nicolas, A. (1986) Structure and petrology of peridotites: clues to their geodynamic environment. *Rev. Geophys.*, **24**, 875–95.

Nicolas, A. (1989) *Structures of Ophiolites and Dynamics of Oceanic Lithosphere.* Kluwer Academic Publishers, Dordrecht, 367 pp.

Nicolas, A. and Prinzhofer, A. (1983) Cumulative or residual origin for the transition zone in ophiolites: structural evidence. *J. Petrol.*, **24**, 188–206.

Pearce, J.A., Lippard, S.J. and Roberts, S. (1984) Characteristics and tectonic significance of supra-subduction zone ophiolites. In *Marginal Basin Geology* (B.P. Kokelaar and M.F. Howells, eds.).

Geol. Soc. Lond. Spec. Publ., **16**, 77–94.

Quick, J.E. (1981) The origin and significance of large, tabular dunite bodies in the Trinity peridotite, northern California. *Contrib. Mineral. Petrol.*, **78**, 413–22.

Roeder, P.L. and Campbell, I.H. (1985) The effect of postcumulus reactions on composition of chrome-spinels from the Jimberlana intrusion. *J. Petrol.*, **26**, 763–86.

Shibata, T. (1976) Phenocryst-bulk rock composition relations of abyssal tholeiites and their petrogenetic significance. *Geochim. Cosmochim. Acta*, **40**, 1407–17.

Shido, F., Miyashiro, A. and Ewing, M. (1971) Crystallization of abyssal tholeiites. *Contrib. Mineral. Petrol.*, **31**, 251–66.

Suhr, G. (1991) *Structural and magmatic history of upper mantle peridotites in the Bay of Islands Complex, Newfoundland.* Unpubl. Ph.D. thesis, Memorial University of Newfoundland, Canada.

Suhr, G. and Robinson, P.T. (1994) Origin of mineral chemical stratification in the mantle section of the Table Mountain massif (Bay of Islands ophiolite, Newfoundland, Canada). *Lithos*, **31**, 81–102.

Violette, J.-F. (1980) *Structure des ophiolites des Philippines (Zambales et Palawan) et de Chypre. Ecoulement asthénosphérique sous les zones d'expansion océaniques.* Unpubl. Thèse Doctorat 3ème cycle, Université de Nantes, France.

Watson, E.B. (1982) Melt infiltration and magma evolution. *Geology*, **10**, 236–40.

[*Revised manuscript received 10 July 1995*]

APPENDIX I. Samples examined from ODP Leg 147 Hole 895D

Sample[1]	Unit	Rock type
01R-01 031-036 #06	1	Harzburgite
02R-01 038-041 #06A	3	Harzburgite
02R-02 008-012 #01B	3–4	Harzburgite-dunite contact
03R-01 038-043 #06D	5	Harzburgite
04R-02 069-072 #11	6	Dunite
04R-02 118-121 #18	7	Harzburgite
04R-02 134-139 #19	7	Harzburgite
04R-03 093-096 #11	7	Harzburgite
05R-02 090-095 #13	9	Harzburgite
07R-01 050-052 #08	14	Troctolite
07R-01 086-091 #14	14	Troctolite
07R-01 105-110 #18	15	Harzburgite in dunite
07R-02 084-089 #11	19	Harzburgite
07R-03 013-016 #02	19	Harzburgite
08R-01 048-051 #07	21	Harzburgite
08R-01 065-073 #10	25	Troctolite
08R-01 092-097 #14	27	Dunite (serpentinite)
08R-02 009-012 #01	31	Gabbro
09R-01 014-018 #03	36	Dunite (serpentinite)
09R-01 028-035 #05	37	Harzburgite (serpentinite)
10W-01 021-026 #03	Washing	Dunite (serpentinite)
10W-01 054-061 #07	Washing	Troctolite

[1]Notation for sample is core number (R = rotary core, W = washing), section number (each section is a maximum length of 1.50 m), depth in cm from top of section, piece number.